

**Climatology, seasonality and trends of oceanic coherent
eddies**

Josué Martínez-Moreno¹, Andrew McC. Hogg¹, and Matthew England²

⁴ Research School of Earth Science and ARC Center of Excellence for Climate Extremes, Australian
⁵ National University, Canberra, Australia

⁶ Climate Change Research Centre (CCRC), UNSW Australia, Sydney NSW, Australia

Key Points:

- ⁸ Kinetic energy of coherent eddies contain around 30% of the surface ocean kinetic
⁹ energy budget.
- ¹⁰ Seasonal cycle of the number of coherent eddies and coherent eddy amplitude re-
¹¹ veal a 3-6 month lag to wind forcing
- ¹² The coherent eddy amplitude has increase at a rate of 3 cm per decade since 1993.

13 Abstract

Ocean eddies influence regional and global climate through mixing and transport of heat and properties. One of the most recognizable and ubiquitous feature of oceanic eddies are vortices with spatial scales of tens to hundreds of kilometers, frequently referred as “mesoscale eddies” or “coherent eddies”. Coherent eddies are known to transport properties across the ocean and to locally affect near-surface wind, cloud properties and rainfall patterns. Although coherent eddies are ubiquitous, yet their climatology, seasonality and long-term temporal evolution remains poorly understood. Thus, we examine the kinetic energy contained by coherent eddies and we present the annual, interannual, and long-term changes of automatically identified coherent eddies from satellite observations and a state of the art numerical simulation from 1993 to 2018. Satellite observations show that around 40% of the kinetic energy contained by ocean eddies corresponds to coherent eddies. Additionally, a strong hemispherical seasonal cycle is observed, on top of a 3–6 months lag between the wind forcing and the response of the coherent eddy field. Furthermore, the seasonality of the number of coherent eddies and their amplitude reveals that the number of coherent eddies responds faster to the forcing (~ 3 months), while the coherent eddy amplitude is lagged by ~ 6 months. There are regions that show a pronounced influence of coherent eddies, notably, the East Indian Ocean, the East Tropical Pacific Ocean, and the South Atlantic Ocean. In these locations, a strong seasonal cycle and interannual variability can be observed in both satellite and numerical models. Although, there is agreement between these products on the seasonality of the number of eddies, the seasonality of the coherent eddy amplitude between these products show some inconsistencies. Long-term trends of the coherent eddy amplitude from satellite observations and the state of the art model show significant increases in the eddy amplitude of $\sim 3\text{cm}$ per decade in large portions of the ocean, while the number of coherent eddies remains constant. Our analysis highlight the relative importance of the coherent eddy fiend in the ocean kinetic energy budget, imply a strong response of the eddy number and eddy amplitude to the surface wind at different time-scales, and showcases for the first time seasonality, and multidecadal trends of the coherent eddy properties.

42 Plain language summary

43 **1 Introduction**

44 Mesoscale ocean variability with spatial scales of tens to hundreds of kilometers is
 45 comprised by processes such as vortices, waves, and jets (Ferrari & Wunsch, 2009; Wyrtki
 46 et al., 1976). These mesoscale processes

47 energetic scale in the ocean and plays a crucial role in the transport of heat, salt,
 48 momentum and other tracers through the ocean. In particular, one of the most rec-
 49 ognizable and abundant mesoscale process are vortices (Abernathay & Marshall, 2013;
 50 Chelton et al., 2011). Although, in literature mesoscale vortices are commonly refer as
 51 "mesoscale eddies", this term is often used to describe mesoscale ocean variability, thus,
 52 we will refer to coherent vortices as coherent eddies. Coherent eddies are circular cur-
 53 rents in the ocean, they are ubiquitous in the oceans, and they

54 Baroclinic generation (Flierl et al., 1980)

55 The term "mesoscale eddy" applied to a rotating coherent structure of ocean cur-
 56 rents that resembles an atmospheric storm, generally refers to ocean signals with spa-
 57 tial scales from tens to hundreds of kilometers and temporal scales from days to months
 58 (Robinson, 2010). Eddies can be found nearly everywhere in the world ocean (Abernathay
 59 and Marshall, 2013; Chelton et al., 2011b), and they transport water, heat, salt, and en-
 60 ergy as they propagate in the ocean (Dong et al., 2014; Roemmich and Gilson, 2001; Thomp-
 61 son et al., 2014; Xu et al., 2011). Eddies also play a significant role in transferring sol-
 62 uble carbon, chlorophyll, nutrients, and other tracers across the ocean, and have impor-
 63 tant influences on the marine ecosystem (Adams et al., 2011; Chelton et al., 2011a; Gaube,
 64 2013). By combining satellite altimetry and Argo profiling float data, Zhang et al. (2014)
 65 found that eddy-induced zonal mass transport was comparable in magnitude to that of
 66 the large-scale wind- and thermohaline-driven circulation.

67 In many previous studies, eddies have been treated as independent water bodies
 68 without consideration of eddy-eddy interaction. In fact, eddy-eddy interaction is uni-
 69 versal within the ocean (Trieling et al., 2005; Prants et al., 2011). Some studies for eddy-eddy
 70 interaction have found plenty of multicore eddy structures within the world ocean (Li
 71 and Sun, 2015; Trieling et al., 2005; Yi et al., 2015). Generally, multicore structures, which
 72 have two or more closed eddies of the same polarity within their boundaries, represent
 73 an important transitional stage in which the component eddies might experience split-

ting, merging, or other energy-transferring interactions. In studying eddy–eddy interaction processes, clear identification of multicore eddy structures is necessary. Chelton et al. (2011b) used a purely geometric method that based on sea level anomaly (SLA) to identify the global eddies, and recognized that their original identification algorithm can yield eddies with more than one local extremum of SLA. Note that such multiple eddies are very common in SLA data (Li and Sun, 2015; Wang et al., 2015), this problem can occur when multiple eddies are physically close together. For these multiple eddies, Yi et al. (2015) presented a Gaussian-surface-based approach to identify and characterize the multicore structures of eddies from SLA datasets and results of detecting dual-eddy structures in the South China Sea demonstrate the effectiveness of the identification approach.

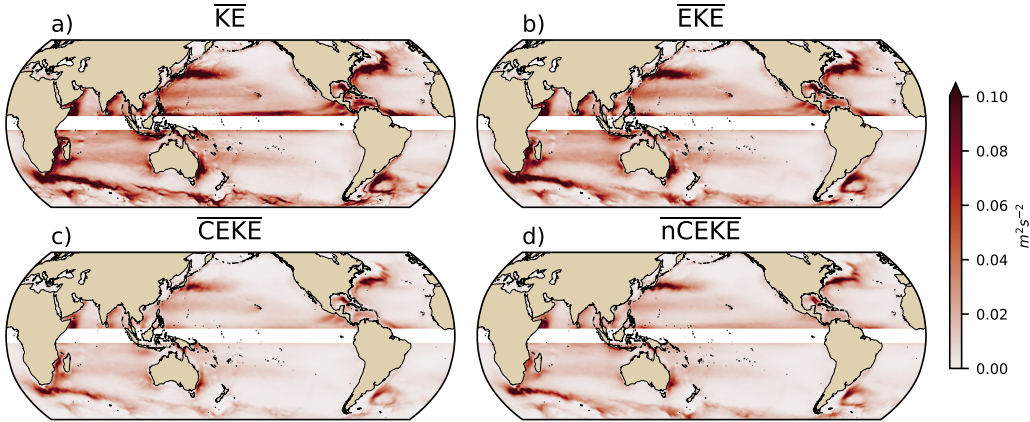
Here we compute global climatology focusing in the spatial distribution instead of the purely seasonality cycle. The main goal of the present work is to generate a global climatology from the latest satellite observation dataset available, in order to complement the known information of the variability of the superficial Kinetic Energy. The data sources and methodology are described in section 2. Global seasonality, inter-annual variability and trends are explored in sections ??, ??, and ?? respectively. In section ?? we present four regions in which we further investigate the temporal variability of kinetic energy and each of its components.

2 Methods

2.1 Kinetic Energy decomposition

Kinetic energy is commonly divided into the mean and temporal variability components through a Reynolds decomposition. At a given time, the velocity field (\mathbf{u}) is split into the time mean ($\bar{\mathbf{u}}$) and time varying components (\mathbf{u}'). Additionally, as part of the climatology we also further decompose the eddy kinetic energy into the eddy kinetic energy contained by coherent features (\mathbf{u}'_e) and non-coherent (\mathbf{u}'_n). Therefore the KE equation can be written as:

$$\text{KE} = \bar{\mathbf{u}}^2 + \underbrace{\mathbf{u}'_e^2 + \mathbf{u}'_n^2}_{\mathbf{u}'^2} + \mathcal{O}^2 \quad (1)$$



113 **Figure 1.** Climatology of surface kinetic energy (\overline{KE}), surface eddy kinetic energy (\overline{EKE}),
114 surface coherent eddy kinetic energy (\overline{CEKE}), and surface non-coherent eddy kinetic energy
115 (\overline{nCEKE}) between 1993–2018.

101 The second order terms (\mathcal{O}) are negligible as their time average is two orders of mag-
102 nitude smaller than any other term. For more information about the decomposition of
103 the field into coherent features and non-coherent features refer to Martínez-Moreno et
104 al. (2019).

105 3 Results

106 3.1 Coherent Eddy Energetics

107 3.1.1 Global

108 **Figure 1**

- 109 • All KE components have large energy contents in the boundary currents and antarc-
110 tic circumpolar current.
- 111 • There are several regions where the coherent component is larger than the non-
112 coherent, we will investigate these in more detail in section XX.

116 **Figure 2**

- 117 • \overline{EKE} is responsible of almost all the \overline{KE} across the ocean, except for regions with
118 persistent currents over time, such as the mean boundary current locations, equa-

- 119 torial pacific currents and regions in the Antarctic Circumpolar current, where the
 120 EKE explains around 40% of the \overline{KE}
 121 • \overline{EKE} Explains 80% of \overline{KE} , while \overline{CEKE} is 45% of \overline{EKE} and \overline{nCEKE} is 60% of
 122 \overline{EKE}
 123 • \overline{CEKE} is large equatorwards from the Kuroshio current and Agulhas current.
 124 • Areas with the largest coherent contribution are located in the South of Australia
 125 \overline{CEKE} and South Atlantic
 126 •
 127 • \overline{nCEKE} has a large amount of energy at high latitudes, this could be a consequence
 128 of the satellites not resolving the mesoscale coherent eddies.
 129 • Global averages of the ratios show \overline{EKE} explains around 78% of the ocean *MKE*
 130 field, while coherent eddies and non coherent eddy features contain 49% and 59%
 131 per decade. Note this values don't add to 100% as there are cross terms that con-
 132 tain around XX% of the total energy.
 133 •

141 **3.1.2 Seasonality**

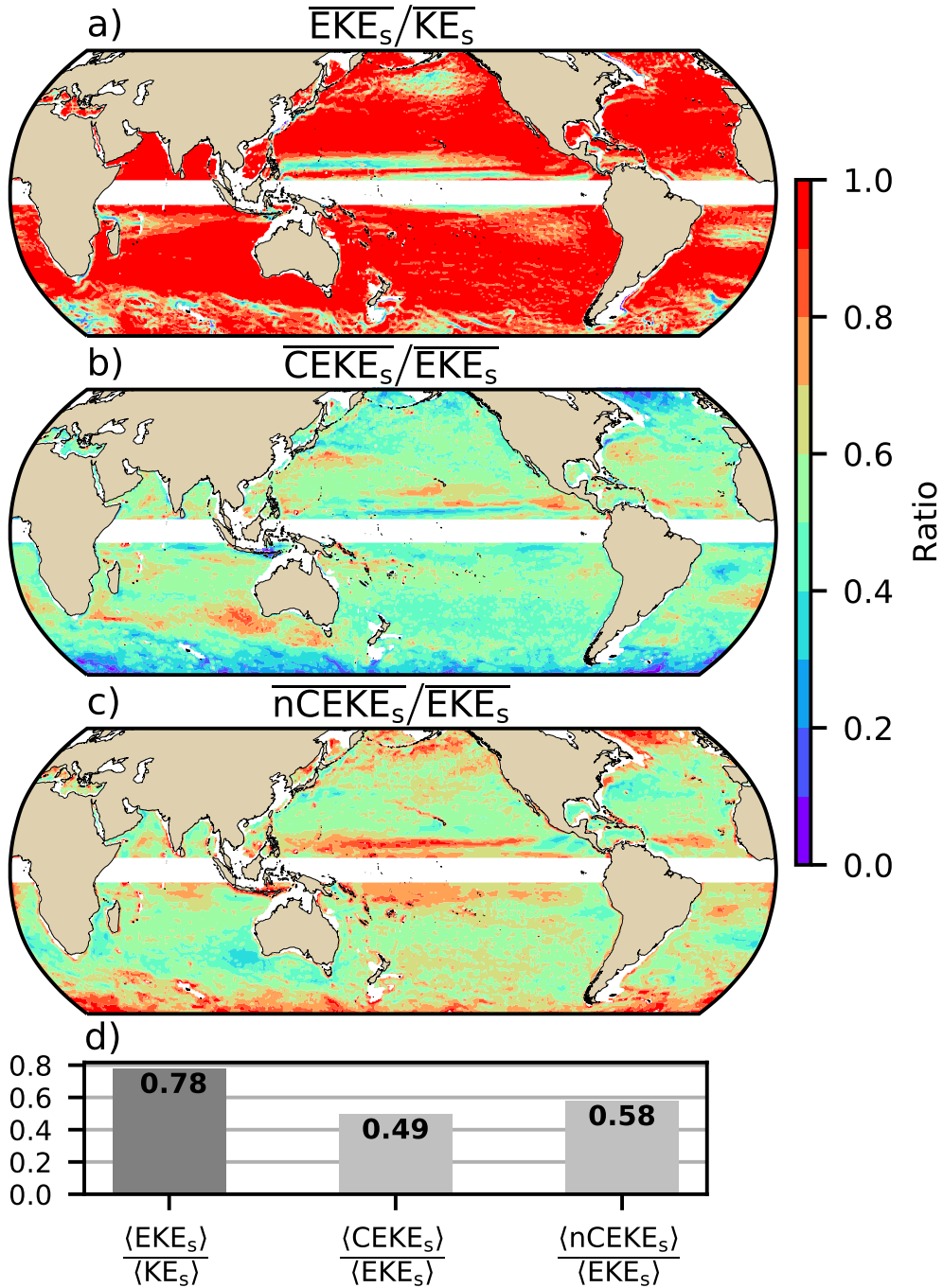
142 **Figure 3**

- 143 • The hemisphere seasonality show the EKE and CEKE peak in summer.
 144 • Response of the EKE and CEKE show a seasonal lag of \sim 6 months to the forc-
 145 ing of the Winds.
 146 • The coherent eddy field show a large interannual variability.
 147 • In the Southern Ocean we observe a concentric growth as time passes, which sup-
 148 port the increasing trends in the Southern Ocean observed by (Hogg et al., 2015;
 149 Martínez-Moreno et al., 2019, 2021)

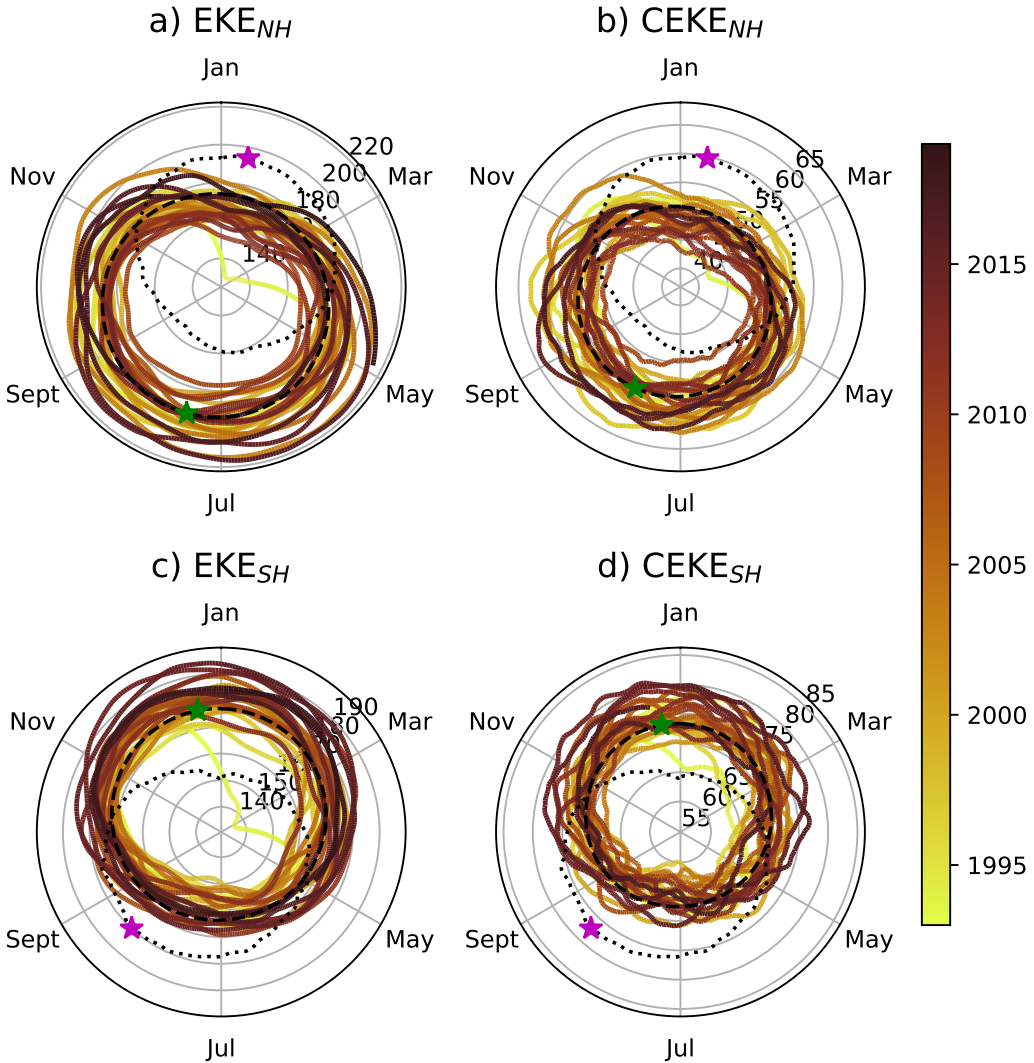
157 **3.2 Coherent Eddy Statistics**

158 **3.2.1 Global**

159 **Figure 4**



134 **Figure 2.** Ratios of the kinetic energy components. a) Map of the proportion of mean eddy
 135 kinetic energy (EKE) versus mean kinetic energy (\overline{KE}); b) Map of the proportion of mean co-
 136 herent eddy kinetic energy (\overline{CEKE}) versus mean eddy kinetic energy (\overline{EKE}); c) Map of the
 137 proportion of mean non-coherent eddy kinetic energy (\overline{nCEKE}) versus mean eddy kinetic energy
 138 (\overline{EKE}); d) Global ratios of mean eddy kinetic energy ($\langle \overline{EKE} \rangle$), mean coherent eddy kinetic en-
 139 ergy ($\langle \overline{CEKE} \rangle$) and mean non coherent eddy kinetic energy ($\langle \overline{nCEKE} \rangle$) versus the global mean
 140 kinetic energy ($\langle \overline{KE} \rangle$) and global mean eddy kinetic energy ($\langle \overline{EKE} \rangle$).



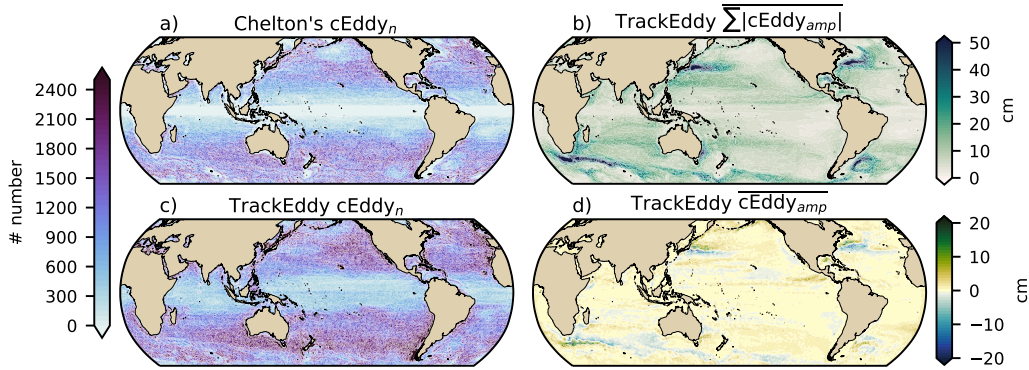
150 **Figure 3. Fix labels** Hemispherical seasonality of eddy kinetic energy (EKE), coherent eddy
 151 kinetic energy (CEKE), and non-coherent eddy kinetic energy (CEKE). Panels a,b and c show
 152 the northern hemisphere seasonal cycle, while panels d,e, and f correspond to the southern hemi-
 153 sphere. Dashed lines correspond to the seasonal climatology of the fields and dotted lines show
 154 the climatology of the wind magnitude. The green and magenta stars show the maximum of the
 155 seasonal cycle for the kinetic energy components and the wind magnitude, respectively. The line
 156 colors show the year.

- A comparison with previous identified numbers show a consistent pattern in the eddy count. The difference in the magnitude could be a consequence of Chelton et al. (2007) filtering the coherent eddies with lifespans longer than 16 weeks.
- Both datasets show a large number of eddies in the East North Pacific, East North Atlantic, as well as the East South Pacific, East South Atlantic and East Indian Ocean.
- While the number of eddies detected in the tropics is quite small.
- Furthermore, there are hotspots of numbers of eddies in other regions of the ocean, such as boundary currents and the Antarctic Circumpolar Current.
- An interesting feature shown in both datasets is a predominant patchiness where the count of the eddies is much larger. These puzzling pattern remains unknown. Although it looks like a propagation pattern, it could be that eddies persist for longer in those areas.
- The eddy amplitude as expected is maximum at the boundary currents and hotspots in the southern ocean.
- Interior of the gyres we can observe that there is an important amplitude of the coherent eddy field.
- Preferred eddy amplitude sign in boundary currents; positive amplitude polewards to the boundary current mean location, and negative amplitude equatorwards. This is consistent with the shed of coherent eddies from the boundary currents.
- There regions with large CEKE ratio show also a large coherent eddy amplitude.

3.2.2 Seasonality

Figure 5

- Seasonality of the number of eddies in the Northern Hemisphere peaks on May, while the Southern Hemisphere peaks on October.
- The seasonality of the amplitude of the eddies is consistent with those of the Coherent eddy kinetic energy.
- Interestingly, there is a 3 month lag between the winds and the seasonality of the number of eddies, while the eddy amplitude responds approximately 6 months after the maximum winds.
- Note that both coherent eddy amplitudes seem to peak around the same time.



181 **Figure 4.** Climatology of the coherent eddy statistics. a) Climatology of the number of coherent
 182 eddies ($cEddy_n$) identified by Chelton et al. (2007); b) Climatology of the warm core coherent
 183 eddy amplitude ($cEddy_{amp}$). c) Climatology of the number of coherent eddies ($cEddy_n$) identi-
 184 fied by Martínez-Moreno et al. (2019); d) Climatology of the cold core coherent eddy amplitude
 185 ($cEddy_{amp}$).

- 196 • If we look closely, the growing-shrinking concentric circles correspond to an increasing-
 197 decreasing trend. These are particularly obvious as a decrease in the eddy num-
 198 ber in the Southern Hemisphere, and a increase in the eddy amplitude.

208 3.3 Regional

209 **Figure 6**

- 210 • a

219 **Figure 7**

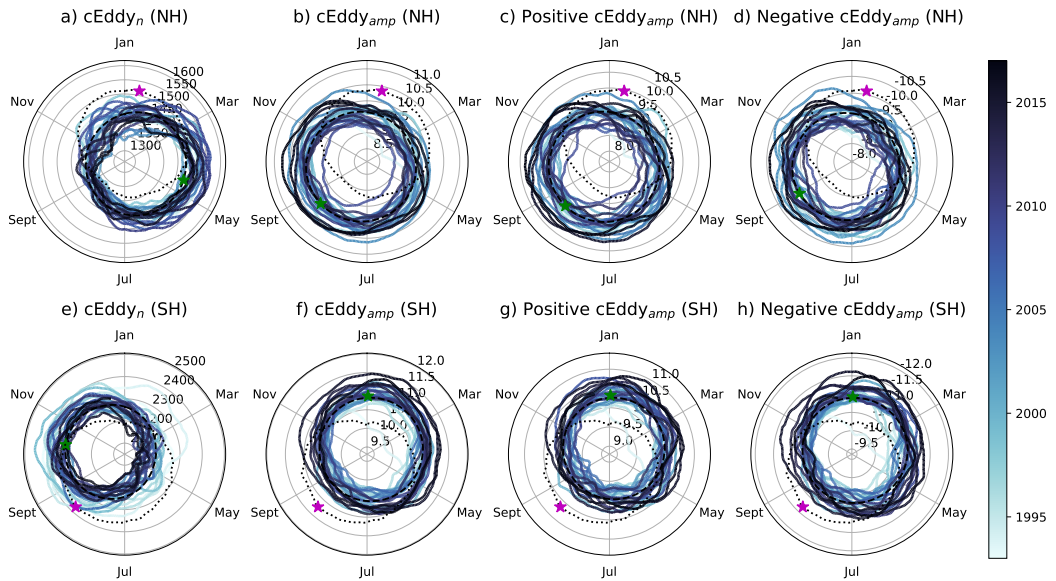
- 220 • a

230 **Figure 8**

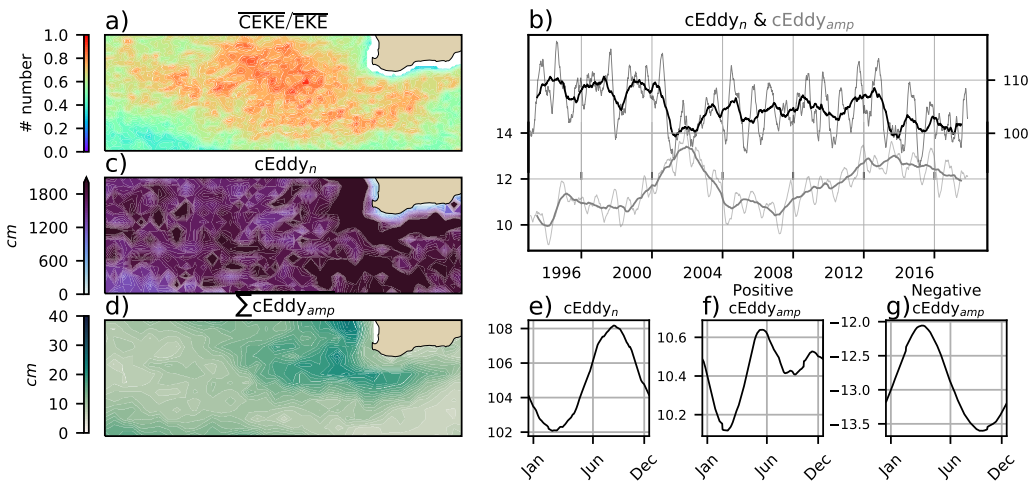
- 231 • a

241 **Figure 9**

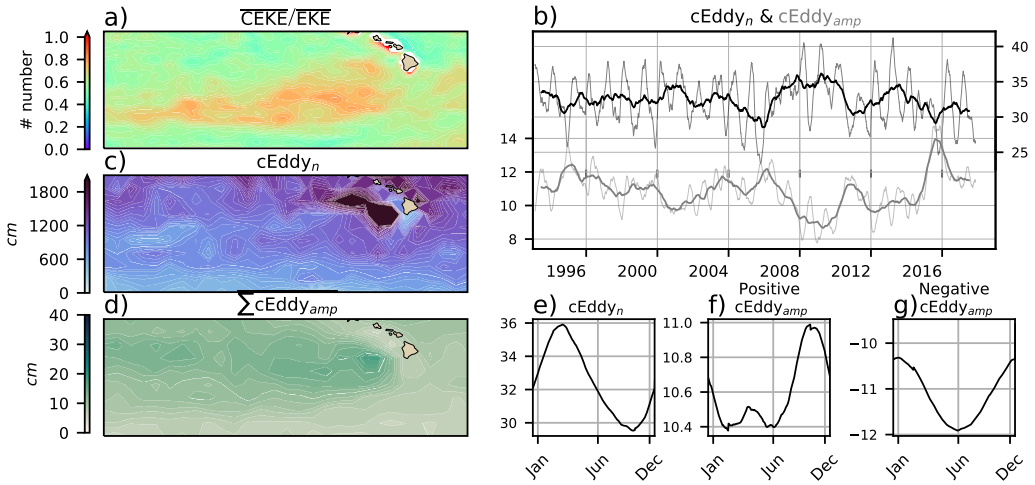
- 242 • a



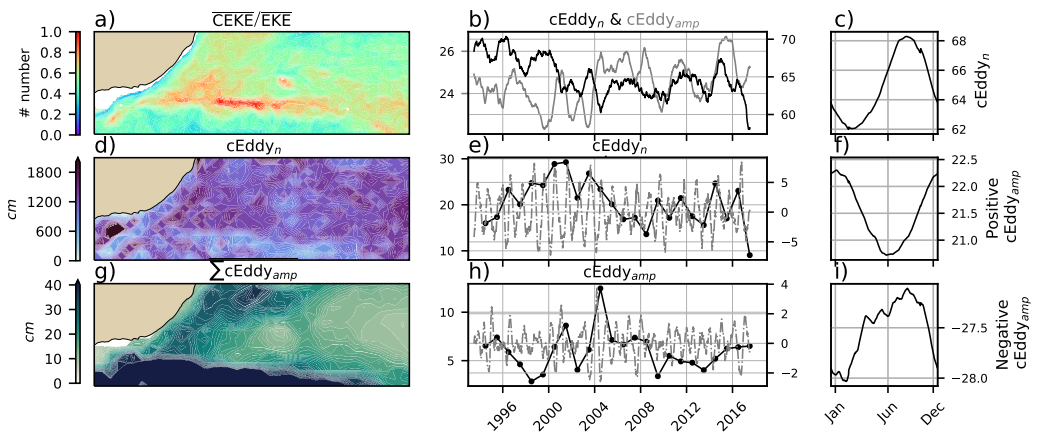
199 **Figure 5.** Hemispherical seasonality of the coherent eddy statistics; a,e) seasonal cycle of the
 200 number of coherent eddies ($cEddy_n$); b,f) seasonal cycle of the mean coherent eddy amplitude
 201 ($cEddy_{amp}$); c,g) seasonal cycle of the warm core coherent eddies amplitude ($wcEddy_{amp}$); d,h)
 202 seasonal cycle of the cold core coherent eddies amplitude ($ccEddy_{amp}$). Panels a,b and c show
 203 the northern hemisphere seasonal cycle, while panels d,e, and f correspond to the southern hemi-
 204 sphere. Dashed lines correspond to the seasonal climatology of the fields and dotted lines show
 205 the climatology of the wind magnitude. The green and magenta stars show the maximum of the
 206 seasonal cycle for the kinetic energy components and the wind magnitude, respectively. The line
 207 colors show the year.



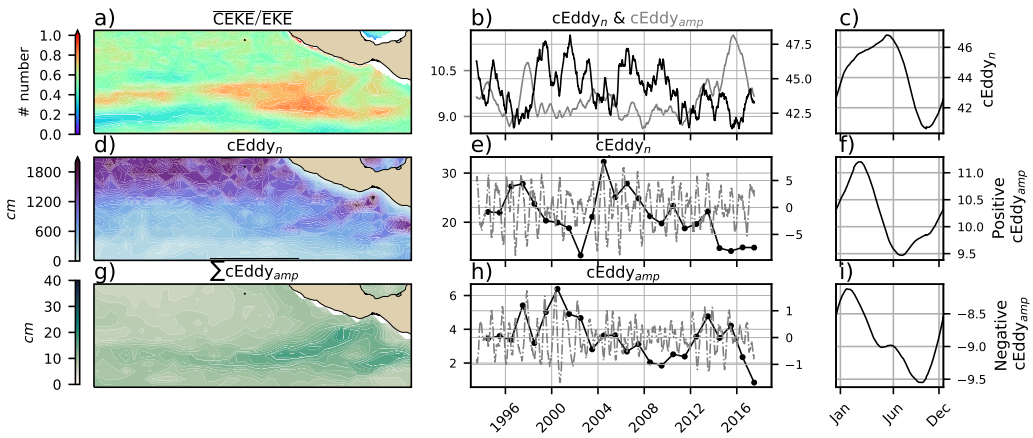
211 **Figure 6.** Climatology of the eddy field and coherent eddy field for the East Indian Ocean. a)
 212 Ratio of mean coherent eddy kinetic energy ($\overline{\text{CEKE}}$) versus mean eddy kinetic energy ($\overline{\text{EKE}}$); b)
 213 Running average over 10 years of the coherent eddy number and amplitude; c) Seasonal cycle of
 214 the number of eddies; d) Map of the number of eddies; e) Multi decadal oscillation of the coher-
 215 ent eddy number; f) Seasonal cycle of the warm core eddies; g) Map of the sum of the absolute
 216 coherent eddy amplitudes; h) Multi decadal oscillation of the coherent eddy number; h) Seasonal
 217 cycle of the cold core eddies. Multi decadal oscillations are defined as the difference between a 2
 218 year running average and a 10 year running average; f) Seasonal cycle of the warm core eddies.



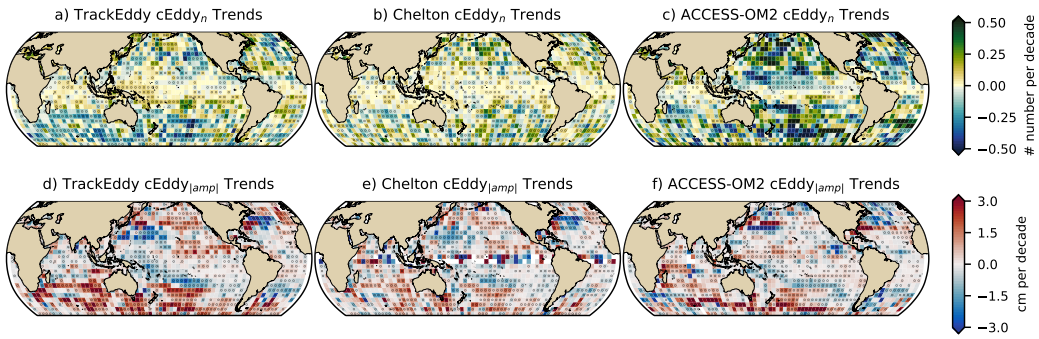
221 **Figure 7.** Climatology of the eddy field and coherent eddy field for the central north pacific.
222 a) Ratio of mean coherent eddy kinetic energy ($\overline{CEKE}/\overline{EKE}$) versus mean eddy kinetic energy (\overline{EKE});
223 b) Running average over 10 years of the coherent eddy number and amplitude; c) Seasonal cy-
224 cle of the number of eddies; d) Map of the number of eddies; e) Multi decadal oscillation of the
225 coherent eddy number; f) Seasonal cycle of the warm core eddies; g) Map of the sum of the ab-
226 solute coherent eddy amplitudes; h) Multi decadal oscillation of the coherent eddy number; h)
227 Seasonal cycle of the cold core eddies. Multi decadal oscillations are defined as the difference
228 between a 2 year running average and a 10 year running average; f) Seasonal cycle of the warm
229 core eddies.



232 **Figure 8.** Climatology of the eddy field and coherent eddy field for the Agulhas retroflexion.
 233 a) Ratio of mean coherent eddy kinetic energy ($\overline{CEKE}/\overline{EKE}$);
 234 b) Running average over 10 years of the coherent eddy number and amplitude; c) Seasonal cy-
 235 cle of the number of eddies; d) Map of the number of eddies; e) Multi decadal oscillation of the
 236 coherent eddy number; f) Seasonal cycle of the warm core eddies; g) Map of the sum of the ab-
 237 solute coherent eddy amplitudes; h) Multi decadal oscillation of the coherent eddy number; h)
 238 Seasonal cycle of the cold core eddies. Multi decadal oscillations are defined as the difference
 239 between a 2 year running average and a 10 year running average; f) Seasonal cycle of the warm
 240 core eddies.



243 **Figure 9.** Climatology of the eddy field and coherent eddy field for the east tropical pacific.
 244 a) Ratio of mean coherent eddy kinetic energy ($\overline{\text{CEKE}}$) versus mean eddy kinetic energy (EKE);
 245 b) Running average over 10 years of the coherent eddy number and amplitude; c) Seasonal cy-
 246 cle of the number of eddies; d) Map of the number of eddies; e) Multi decadal oscillation of the
 247 coherent eddy number; f) Seasonal cycle of the warm core eddies; g) Map of the sum of the ab-
 248 solute coherent eddy amplitudes; h) Multi decadal oscillation of the coherent eddy number; h)
 249 Seasonal cycle of the cold core eddies. Multi decadal oscillations are defined as the difference
 250 between a 2 year running average and a 10 year running average; f) Seasonal cycle of the warm
 251 core eddies.



266 **Figure 10.** Trends of coherent eddy statistics. a,b and c Trends of the number of identified
 267 coherent eddies from satellite observations identified using TrackEddy, satellite observations iden-
 268 tified using Chelton's, and state of the art numerical simulation identified using TrackEddy. d,e
 269 and f Trends of the sum of the absolute value of identified coherent eddies amplitude from satel-
 270 lite observations identified using TrackEddy, satellite observations identified using Chelton's, and
 271 state of the art numerical simulation identified using TrackEddy. Gray stippling shows regions
 272 that are statistically significant above the 95% confidence level.

252 Should we add the interannual variability of Chelton's?

253 Overall, we observe a polewards decrease in the number of the eddies. This sup-
 254 ports the idea that the satellite observations are consistent with a continue dataset.

255 4 Trends

256 Figure 10

- 257 • The number and amplitude of coherent eddies from two eddy tracking algorithms
 258 show consistent trend patterns.
- 259 • In particularly, we observe a decrease in the number of eddies in the southern ocean,
 260 as well as sectors in the North Atlantic and North Pacific.
- 261 • Meanwhile the amplitude seems to be increasing in those same regions.
- 262 • Some of these regions have undergone a readjustment to stronger winds, thus the
 263 observed trends in the eddy amplitude suggests an intensification of the coherent
 264 eddy field to an increase in the forcing.
- 265 • This increase is consistent with Martínez-Moreno et al. (2021)

273 **5 Summary and Conclusions**274 **Acknowledgments**275 **References**

- 276 Abernathey, R. P., & Marshall, J. (2013). Global surface eddy diffusivities derived
 277 from satellite altimetry. *Journal of Geophysical Research: Oceans*, 118(2), 901–
 278 916. doi: 10.1002/jgrc.20066
- 279 Chelton, D. B., Gaube, P., Schlax, M. G., Early, J. J., & Samelson, R. M. (2011).
 280 The influence of nonlinear mesoscale eddies on near-surface oceanic chlorophyll.
 281 *Science*, 334(6054), 328-32. doi: 10.1126/science.1208897
- 282 Chelton, D. B., Schlax, M. G., Samelson, R. M., & de Szoeke, R. A. (2007). Global
 283 observations of large oceanic eddies. *Geophysical Research Letters*, 34(15),
 284 L15606. doi: 10.1029/2007GL030812
- 285 Ferrari, R., & Wunsch, C. (2009). Ocean Circulation Kinetic Energy: Reservoirs,
 286 Sources, and Sinks. *Annual Review of Fluid Mechanics*, 41(1), 253–282. doi: 10
 287 .1146/annurev.fluid.40.111406.102139
- 288 Flierl, G., Larichev, V., McWilliams, J., & Reznik, G. (1980). The dynamics of baro-
 289 clinic and barotropic solitary eddies. *Dynamics of Atmospheres and Oceans*, 5(1),
 290 1–41. doi: 10.1016/0377-0265(80)90009-3
- 291 Hogg, A. M., Meredith, M. P., Chambers, D. P., Abrahamsen, E. P., Hughes,
 292 C. W., & Morrison, A. K. (2015). Recent trends in the Southern Ocean
 293 eddy field. *Journal of Geophysical Research: Oceans*, 120(1), 257-267. doi:
 294 10.1002/2014JC010470
- 295 Martínez-Moreno, J., Hogg, A. M., England, M., Constantinou, N. C., Kiss, A. E.,
 296 & Morrison, A. K. (2021). Global changes in oceanic mesoscale currents over the
 297 satellite altimetry record. *Journal of Advances in Modeling Earth Systems*, 0(ja).
 298 doi: 10.1029/2019MS001769
- 299 Martínez-Moreno, J., Hogg, A. M., Kiss, A. E., Constantinou, N. C., & Mor-
 300 rison, A. K. (2019). Kinetic energy of eddy-like features from sea surface
 301 altimetry. *Journal of Advances in Modeling Earth Systems*, 0(ja). doi:
 302 10.1029/2019MS001769
- 303 Wyrtki, K., Magaard, L., & Hager, J. (1976). Eddy energy in the oceans. *Journal of*

304 *Geophysical Research*, 81(15), 2641-2646. doi: 10.1029/JC081i015p02641